



Research article

A kinetic model considering the decline of antibody level and simulation about vaccination effect of COVID-19

Chuanqing Xu, Xiaotong Huang, Zonghao Zhang and Jing'an Cui*

School of Science, Beijing University of Civil Engineering and Architecture, China

* **Correspondence:** Email: cuijingan@bucea.edu.cn.

Abstract: We build a model that consider the falling antibody levels and vaccination to assess the impact of falling antibody levels and vaccination on the spread of the COVID-19 outbreak, and simulate the influence of vaccination rates and failure rates on the number of daily new cases in England. We get that the lower the vaccine failure rate, the fewer new cases. Over time, vaccines with low failure rates are more effective in reducing the number of cases than vaccines with high failure rates and the higher the vaccine efficiency and vaccination rate, the lower the epidemic peak. The peak arrival time is related to a boundary value. When the failure rate is less than this boundary value, the peak time will advance with the decrease of failure rate; when the failure rate is greater than this boundary value, the peak time is delayed with the decrease of failure rate. On the basis of improving the effectiveness of vaccines, increasing the vaccination rate has practical significance for controlling the spread of the epidemic.

Keywords: COVID-19; epidemic dynamics; SEIR model; vaccine efficiency

1. Introduction

It has been almost two years since the outbreak of COVID-19. A large number of international research results have given us a certain understanding of the virus. This is a severe respiratory illness caused by the coronavirus [1, 2]. The International Committee on Taxonomy of viruses named the virus SARS-CoV-2 is mainly transmitted through respiratory tract. The clinical symptoms of infected people are mostly fever, dry cough and fatigue, and some patients are asymptomatic infected people. When the disease is serious, it will also cause organ failure and even death [3, 4].

Currently, the COVID-19 pandemic is still ongoing. According to the latest outbreak of the World Health Organization, as of October 2021, there were more than 70 million newly confirmed cases in Europe [5]. The United Kingdom is one of the worst-affected countries in Europe, with more than 8 million cumulative cases, of which more than 7 million were diagnosed in England alone [6],

accounting for 85% of the total cumulative cases reported in the United Kingdom.

Since more than 80% of confirmed cases in Britain are concentrated in England, we intend to do some theoretical research based on the data of England for the reference of government decision-making. Figure 1 shows the daily new cases data of COVID-19 epidemic in England during 2020 [6]. In early March, due to the obvious increase of new cases, the British government began to implement the first large-scale social blockade at the end of March and gradually unsealed at the beginning of June. This phase corresponds to the phase in which the first small peak appears in Figure 1. In the three months after the first unsealing, the epidemic situation in the region had been relatively gentle. However, since September, the number of new cases per day had increased significantly. By the end of October, the number of new cases per day had reached about 20000. At this time, the British government once again announced that it would implement the second large-scale social blockade on November 5, which lasted until December 2nd. Soon after the second unsealing, the third wave of more large-scale epidemic began, and there were reports that a mutant virus with stronger transmission ability was detected, and the epidemic reached a stage that was difficult to control. On December 20th, Britain ushered in the third social blockade, which lasted until February 2021.

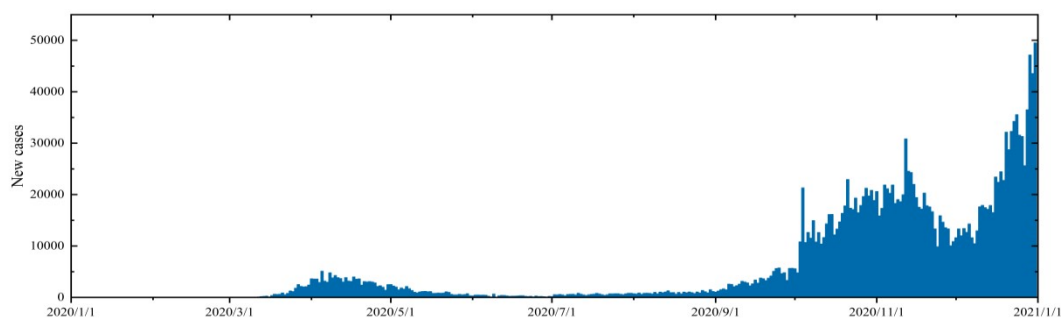


Figure 1. Daily new cases data of COVID-19 in England in 2020.

H. Ward et al. based on antibody levels in 365,000 people, showed that at the start of the second wave of infections in England, only 4.4% of adults had IgG antibodies detected using test for lateral flow immunoassay (LFIA) [7]. A study on the antibody positive rate of asymptomatic and symptomatic infected people in Wanzhou District of Chongqing by Quanxin Long et al showed that after 8 weeks of infection, the antibody concentration of more than 90% of the participants decreased by more than 70% [8]. A study on the neutralizing antibody level of SARS-CoV-2 patients within three months after infection found that after analyzing the serum samples of 65 SARS-CoV-2 infected patients, 95% of the cases had seroconversion [9]. Some researchers found that the antibody titers of the two virus strains decreased significantly, and the delta variant virus strain decreased more significantly than the wild strain [10–12]. The infectious disease dynamics model is a key tool for studying the spread of infectious diseases. It is generally divided into four compartments, susceptible (S), exposed (E), infected (I) and recovered (R) compartments. It can clearly describe the dynamic relationship between various warehouses in the process of virus transmission, and give relatively accurate predictions on the development trend of infectious diseases. P. Wintachai [13] et al. predicted the change trend of COVID-19

cases over time by establishing SEIR infectious disease dynamics model considering different vaccination rates. A. Fuady [14] et al. established an infectious disease dynamics model considering different vaccination times to explore the inhibitory effect of changes in vaccination time on the spread of covid-19 epidemics. M. Angeli et al. [15] et al introduced SAIVR mathematical model to forecast the covid-19 epidemic evolution during the vaccination campaign by employing a semi-supervised machine learning process. S. Zhai [16] et al. studied an SEIR-type epidemic model with time delay and vaccination control, the vaccination strategy was expressed as a state delayed feedback which was related to the current and previous state of the epidemic model and investigated the non-negativity and boundedness of the model. J. Medina [17] et al. modeled a trustable and reliable management system based on block chain for vaccine distribution by extending the SEIR model, which included prevention measures such as mask-wearing, social distancing, vaccination rate, and vaccination efficiency. A. Karabay [18] et al. presented a particle-based SEIR epidemic simulator as a tool to assess the impact of different vaccination strategies on viral propagation and to model sterilizing and effective immunization outcomes and the simulator included modules to support contact tracing of the interactions amongst individuals and epidemiological testing of the general population. J. Wieland [19] et al. developed a model for the simulation of the SARS Cov-2 spread in Germany in the context of a complementary course at the Leuphana University. It tried to simulate different scenarios of the number of cases with the help of ODE. Chen [20] et al. used compartmental models to model and analyze the COVID-19 dynamics of different considered populations as susceptible, exposed, infected and recovered compartments (SEIR). They derived control-oriented compartmental models of the pandemic, together with constructive control laws based on the Lyapunov theory. Antibody levels decrease over time after a person recovers from COVID-19, there will be a chance of re-infection with the virus. In the first model, we explore the impact of declining antibody levels on the spread of the COVID-19 epidemic in the UK, taking into account that a certain proportion of recoveries would become susceptible again. In the optimized model, we add the vaccinated compartment and study the impact of the vaccine's effect on the outbreak.

This study selects the daily new data of the COVID-19 epidemic in England from September 1 to October 31, 2020 as the data for model fitting, that is, the data in the middle and early stages of the second wave of the epidemic in England. Based on these possible factors: 1) The first wave of the epidemic has ended, and the level of antibodies in the infected people began to decline; 2) The British government did not have any intervention policy during this period; 3) There was no vaccination during this period; Therefore we used data for this time period when considering the impact of declining antibody levels on the spread of COVID-19 in this model.

2. SEIR model for the decline of antibody level in population

Because the spread of COVID-19 has a long incubation period and the incubation period is contagious, in our model, we consider the incubation period and adopt the SEIR model. We divide the total population N into four categories: susceptible (S), exposed (E), infected (I), and recovered (R). β is the rate of disease transmission, σ is the conversion rate from exposed people to infected people, γ is the disease recovery rate, μ is the mortality due to disease, and P is the conversion rate from recovered group to susceptible group. The SEIR infectious disease dynamics model considering the decline of antibody level is shown in Figure 2.

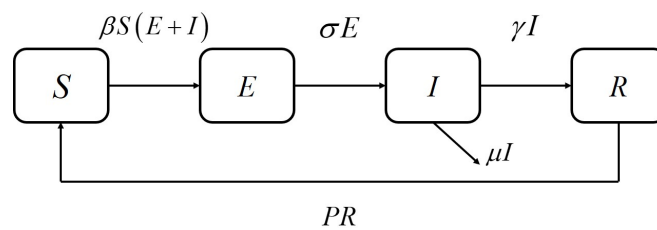


Figure 2. Diagram of COVID-19 transmission considering declining antibody levels.

According to the above COVID-19 spread diagram, we establish the infectious disease dynamics model as follows:

$$\begin{cases} \frac{dS}{dt} = -\beta S(E+I) + PR, \\ \frac{dE}{dt} = \beta S(E+I) - \sigma E, \\ \frac{dI}{dt} = \sigma E - (\mu + \gamma)I, \\ \frac{dR}{dt} = \gamma I - PR. \end{cases} \quad (2.1)$$

2.1. Equilibrium point of the model

We obtain, when $I = 0$, the disease-free equilibrium point of model (2.1) is $E_{01} = (S_0, 0, 0, 0)$. When $I \neq 0$, the endemic equilibrium point of model (2.1) is

$$E_1^* = \left(\frac{S_0}{R_0}, \frac{\gamma + \mu}{\sigma} I^*, I^*, \frac{\gamma}{P} I^* \right), I^* \neq 0.$$

2.2. Basic reproduction number

The basic reproduction number refers to the average number of secondary cases after an infected individual enters the susceptible population [21], the next generation matrix is the most commonly used method to calculate the basic reproduction number.

In order to calculate the basic reproduction number of model (2.1), we take

$$\mathcal{F} = \begin{pmatrix} \beta S(E+I) \\ 0 \end{pmatrix}, \mathcal{V} = \begin{pmatrix} \sigma E \\ -\sigma E + (\gamma + \mu)I \end{pmatrix}.$$

The Jacobian matrices of \mathcal{F} and \mathcal{V} are

$$F = \begin{pmatrix} \beta S & \beta S \\ 0 & 0 \end{pmatrix}, V = \begin{pmatrix} \sigma & 0 \\ -\sigma & \gamma + \mu \end{pmatrix}.$$

At disease-free equilibrium, we obtain

$$FV^{-1}|_{E_{01}} = \begin{pmatrix} \frac{\beta S_0}{\sigma} + \frac{\beta S_0}{\gamma + \mu} & \frac{\beta S_0}{\gamma + \mu} \\ 0 & 0 \end{pmatrix}.$$

The basic reproduction number \mathcal{R}_0 is the spectral radius of $FV^{-1}|_{E_{01}}$, so the expression is

$$\mathcal{R}_0 = \frac{\beta S_0 (\sigma + \gamma + \mu)}{\sigma (\gamma + \mu)}.$$

2.3. Stability analysis of disease-free equilibrium

Theorem 1. When $\mathcal{R}_0 < 0$, model (2.1) is stable at the disease-free equilibrium point, otherwise unstable.

Proof. The Jacobian matrix of model (2.1) at E_{01} is

$$J|_{E_{01}} = \begin{pmatrix} 0 & -\beta S_0 & -\beta S_0 & 0 \\ 0 & \beta S_0 - \sigma & \beta S_0 & 0 \\ 0 & \sigma & -(\gamma + \mu) & 0 \\ 0 & 0 & \gamma & -P \end{pmatrix}.$$

The matrix eigenvalue satisfies the following formula:

$$\begin{aligned} |\lambda E - J|_{E_{01}}| &= \begin{vmatrix} \lambda & \beta S_0 & \beta S_0 & 0 \\ 0 & \lambda - \beta S_0 + \sigma & -\beta S_0 & 0 \\ 0 & -\sigma & \lambda + \gamma + \mu & 0 \\ 0 & 0 & -\gamma & \lambda + P \end{vmatrix} \\ &= \lambda(\lambda + P) \left[\lambda^2 + (\sigma + \gamma + \mu - \beta S_0) \lambda + \sigma(\gamma + \mu) - \beta S_0(\sigma + \gamma + \mu) \right]. \end{aligned}$$

Obviously $\lambda_1 = 0$, $\lambda_2 = -P < 0$, the other two eigenvalues λ_3 , λ_4 satisfy the equation

$$P(\lambda) = \lambda^2 + a_1 \lambda + a_2 = 0,$$

where

$$a_1 = \sigma + \gamma + \mu - \beta S_0, \quad a_2 = \sigma(\gamma + \mu) - \beta S_0(\sigma + \gamma + \mu).$$

Easy to know

$$\frac{\beta S_0}{\sigma + \gamma + \mu} = \mathcal{R}_0 \frac{\sigma(\gamma + \mu)}{(\sigma + \gamma + \mu)^2} < 1,$$

therefore,

$$\begin{aligned} a_1 &= \sigma + \gamma + \mu - \beta S_0 > 0, \\ a_2 &= \sigma(\gamma + \mu) - \beta S_0(\sigma + \gamma + \mu) = \sigma(\gamma + \mu)(1 - \mathcal{R}_0). \end{aligned}$$

So, when $\mathcal{R}_0 < 1$, we obtain $a_1 > 0$ and $a_2 > 0$. According to Hurwitz discriminant method, the characteristic roots λ_3 , λ_4 of $P(\lambda)$ have negative real parts.

To sum up, among the eigenvalues of the Jacobian matrix of model (2.1), the real part of four eigenvalues is negative and one is zero. So, when $\mathcal{R}_0 < 1$, model (2.1) is stable at the disease-free equilibrium point, otherwise unstable.

3. SEIRV model of vaccination

Antibody levels decline over time, and herd immunity approaches that rely on natural immunity become unfeasible. Therefore, on the basis of the above model (2.1), we add the vaccination compartment (people who were successfully vaccinated) to establish the SEIRV model. In this model, we consider daily vaccination of susceptible populations at a fixed vaccination rate and explore the impact of varying injection and failure rates on the outbreak in England. The propagation mechanism of the model is shown in the Figure 3. Here α refers to the daily proportion of vaccination, ω is the vaccine

failure rate and refers to the reciprocal of the duration of vaccine effectiveness. The other parameters are the same of model (2.1).

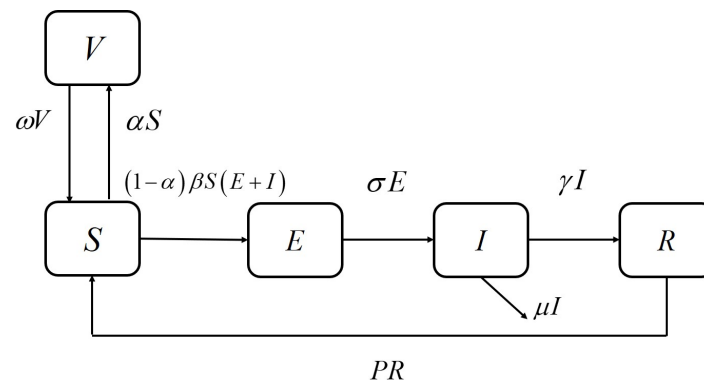


Figure 3. Diagram of COVID-19 transmission considering declining antibody levels and vaccination.

According to the above COVID-19 diagram, the infectious disease dynamics model we established is

$$\begin{cases} \frac{dS}{dt} = -\alpha S - (1-\alpha)\beta S(E+I) + PR + \omega V, \\ \frac{dE}{dt} = (1-\alpha)\beta S(E+I) - \sigma E, \\ \frac{dI}{dt} = \sigma E - (\gamma + \mu)I, \\ \frac{dR}{dt} = \gamma I - PR, \\ \frac{dV}{dt} = \alpha S - \omega V. \end{cases} \quad (3.1)$$

3.1. Equilibrium point of the model

Let

$$\begin{cases} -\alpha S - (1-\alpha)\beta S(E+I) + PR + \omega V = 0, \\ (1-\alpha)\beta S(E+I) - \sigma E = 0, \\ \sigma E - (\gamma + \mu)I = 0, \\ \gamma I - PR = 0, \\ \alpha S - \omega V = 0. \end{cases}$$

When $I = 0$, there are

$$S = S_0, E = 0, R = 0, V = \frac{\alpha S_0}{\omega}.$$

The disease-free equilibrium point of model (3.1) is

$$E_{02} = (S_0, 0, 0, 0, \frac{\alpha S_0}{\omega}).$$

When $I \neq 0$, we obtain

$$S^* = \frac{S_0}{\mathcal{R}_0}, E^* = \frac{\gamma + \mu}{\sigma} I^*, R^* = \frac{\gamma}{P} I^*, V^* = \frac{\alpha S_0}{\omega \mathcal{R}_C}.$$

Therefore, the endemic equilibrium point of model (3.1) is

$$E_2^* = \left(\frac{S_0}{\mathcal{R}_C}, \frac{\gamma + \mu}{\sigma} I^*, I^*, \frac{\gamma}{P} I^*, \frac{\alpha S_0}{\omega \mathcal{R}_C} \right), I^* \neq 0.$$

3.2. Control reproduction number

The number of controlled reproduction refers to the number of people who can be infected by an infected person during the infection period under certain prevention and control measures [22]. It is also calculated by the method of next generation matrix.

In order to calculate the control reproduction number of model (3.1), we take

$$\mathcal{F} = \begin{pmatrix} (1-\alpha)\beta S(E+I) \\ 0 \end{pmatrix}, \mathcal{V} = \begin{pmatrix} \sigma E \\ -\sigma E + (\gamma + \mu)I \end{pmatrix}.$$

The Jacobian matrices of \mathcal{F} and \mathcal{V} are

$$F = \begin{pmatrix} (1-\alpha)\beta S & (1-\alpha)\beta S \\ 0 & 0 \end{pmatrix}, V = \begin{pmatrix} \sigma & 0 \\ -\sigma & \gamma + \mu \end{pmatrix}.$$

At disease-free equilibrium, there is

$$FV^{-1}|_{E_{02}} = \begin{pmatrix} \frac{(1-\alpha)\beta S_0}{\sigma} + \frac{(1-\alpha)\beta S_0}{\gamma + \mu} & \frac{(1-\alpha)\beta S_0}{\gamma + \mu} \\ 0 & 0 \end{pmatrix}.$$

The control reproduction number is the spectral radius of $FV^{-1}|_{E_{02}}$, and the expression is

$$\mathcal{R}_C = \frac{(1-\alpha)\beta S_0(\sigma + \gamma + \mu)}{\sigma(\gamma + \mu)}.$$

3.3. Stability analysis of disease-free equilibrium

Theorem 2. When $\mathcal{R}_C < 1$, the model (3.1) is locally asymptotically stable at the disease-free equilibrium point, otherwise it is unstable.

Proof. The Jacobian matrix of model (3.1) at E_{02} is

$$J|_{E_{02}} = \begin{pmatrix} -\alpha & -(1-\alpha)\beta S_0 & -(1-\alpha)\beta S_0 & P & \omega \\ 0 & (1-\alpha)\beta S_0 - \sigma & (1-\alpha)\beta S_0 & 0 & 0 \\ 0 & \sigma & -(\gamma + \mu) & 0 & 0 \\ 0 & 0 & \gamma & -P & 0 \\ \alpha & 0 & 0 & 0 & -\omega \end{pmatrix}.$$

The matrix eigenvalue satisfies the following formula:

$$\begin{aligned} |\lambda E - J|_{E_{02}}| &= \begin{vmatrix} \lambda + \alpha & (1-\alpha)\beta S_0 & (1-\alpha)\beta S_0 & -P & -\omega \\ 0 & \lambda - (1-\alpha)\beta S_0 + \sigma & -(1-\alpha)\beta S_0 & 0 & 0 \\ 0 & -\sigma & \lambda + \gamma + \mu & 0 & 0 \\ 0 & 0 & -\gamma & \lambda + P & 0 \\ -\alpha & 0 & 0 & 0 & \lambda + \omega \end{vmatrix} \\ &= (\lambda + P) \left[\lambda^2 + (\alpha + \omega)\lambda + 2\alpha\omega \right] \\ &\quad \left\{ \lambda^2 + [\sigma + \gamma + \mu - (1-\alpha)\beta S_0]\lambda + \sigma(\gamma + \mu) - (1-\alpha)\beta S_0(\sigma + \gamma + \mu) \right\}. \end{aligned}$$

Obviously $\lambda_1 = -P < 0$, the other eigenvalues λ_2, λ_3 satisfy the equation

$$P_1(\lambda) = \lambda^2 + A_1\lambda + A_2,$$

where

$$A_1 = \omega + \alpha, A_2 = 2\omega\alpha.$$

We obtain

$$\Delta_1 = 1 > 0, \Delta_2 = \begin{vmatrix} A_1 & 1 \\ 0 & A_2 \end{vmatrix} = \begin{vmatrix} \omega + \alpha & 1 \\ 0 & 2\omega\alpha \end{vmatrix} > 0,$$

which means λ_2 and λ_3 have negative real parts. The last two eigenvalues λ_4, λ_5 satisfy the equation

$$P_2(\lambda) = \lambda^2 + B_1\lambda + B_2,$$

where

$$B_1 = \sigma + \gamma + \mu - (1 - \alpha)\beta S_0, B_2 = \sigma(\gamma + \mu) - (1 - \alpha)\beta S_0(\sigma + \gamma + \mu).$$

So, when $\mathcal{R}_C < 1$, we obtain $B_1 > 0$ and $B_2 > 0$. According to Hurwitz discriminant method, the characteristic roots λ_4 and λ_5 have negative real parts.

To sum up, all eigenvalues of the Jacobian matrix of model (3.1) have negative real parts, so model (3.1) is locally asymptotically stable at the disease-free equilibrium point, otherwise it is unstable.

4. Numerical simulation and result

4.1. The parameters in the model

According to model (2.1), the number of new cases per day in England from September 1 to October 31 is fitted by the nonlinear least squares method, and the fitting result is shown in Figure 4. Within the allowable range of error, we set the initial value of the susceptible as $S_0 = 55699400$, the initial value of exposed people as $E_0 = 6500$, the initial value of infected people as $I_0 = 1041$, meaning the number of new cases in England on September 1, and the initial value of recovered people as 200. The conversion rate from exposed people to infected people is $\sigma = 1/12$ (day^{-1}) [23], the recovery rate of disease is $\gamma = 1/14$ (day^{-1}) [24] and the mortality rate is $\mu = 0.003$ [25], which are selected according to the actual transmission of infectious diseases. And we obtain the transmission rate is $\beta = 1.1295 \times 10^{-9}$ and the conversion rate from the recovered group to susceptible group is $P = 1.8888 \times 10^{-6}$ by fitting.

The fitting results of the improved SEIR model are in good agreement with the England data, and can better reflect the growth trend of the COVID-19 epidemic in England.

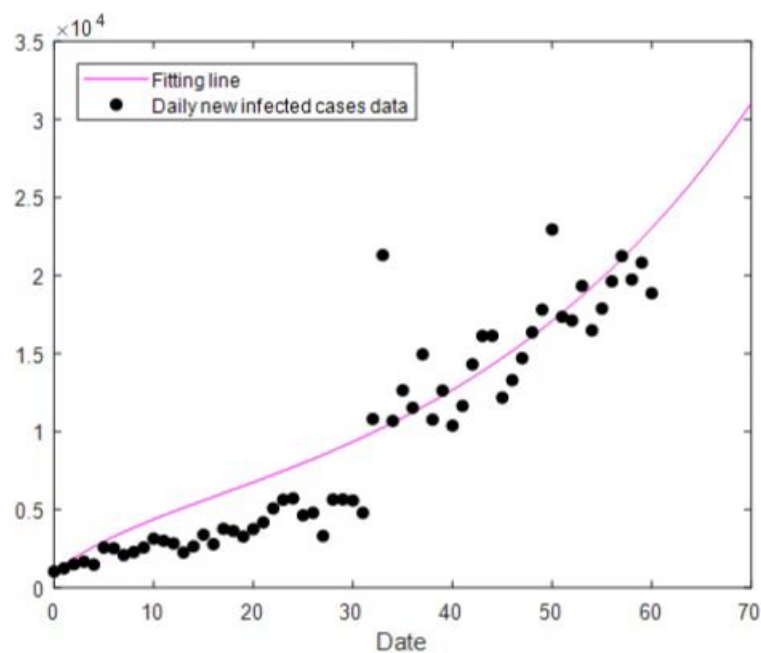


Figure 4. Fitting results for the number of daily new infected cases in England.

In the SEIRV model (3.1), α refers to the daily vaccination rate, which is further explained here. The overall immunization rates corresponding to different daily vaccination rates (60 days after vaccination) is shown in Figure 5. The total population of England is about 50 million, $\alpha = 0.005$ means that 250,000 people are vaccinated on the first day. After 60 days of continuous vaccination, the overall immunization rate is 25.9%.

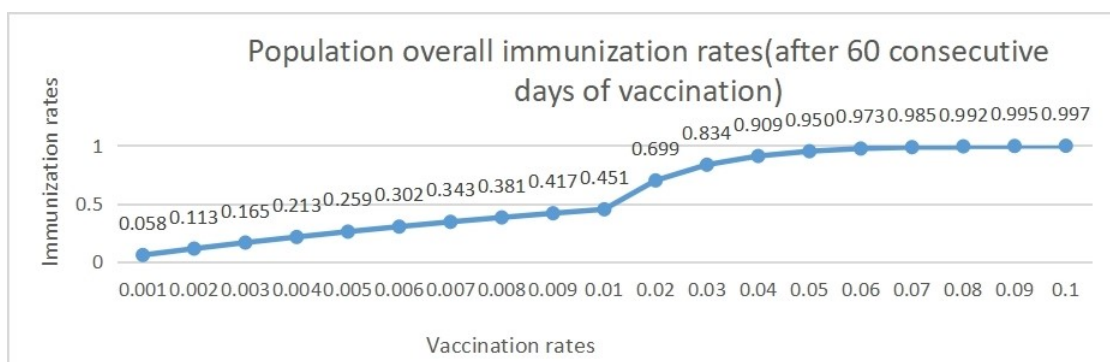


Figure 5. Population overall immunization rates under different vaccination rates (after 60 consecutive days of vaccination).

In SEIRV model, the meaning of vaccine failure rate ω refers to the reciprocal of the duration of vaccine effectiveness, that is, each corresponds to a duration of vaccine effectiveness. The data details are shown in Table 1.

Table 1. Vaccine effective time period corresponding to different vaccine failure rates.

Vaccine failure rates	Vaccine effective time period (days)
0	FOREVER
0.001	1000
0.002	500
0.003	333
0.004	250
0.005	200
0.006	167
0.007	143
0.008	125
0.009	111
0.01	100
0.02	50
0.03	33
0.04	25
0.05	20

4.2. *Effects of different vaccine failure rates on the epidemic situation in England*

In order to evaluate the role of vaccines in epidemic control, we investigate the impact of different vaccination rates and failure rates on the spread of COVID-19 epidemic in England. We change the vaccine failure rate when the fixed vaccination rate is 0.005, and simulate the impact of different failure rates on the spread of COVID-19 epidemic in England. The results are shown in Figures 6 – 8. In Figure 6, the failure rates are taken from 0 to 0.01 in steps of 0.001; in Figure 7, the failure rate is taken from 0.01 to 0.05 in steps of 0.01; in Figure 8, the failure rate is taken from 0.01 to 0.02 in steps of 0.001. As can be seen from Figures 6–8, with the decrease of vaccine failure rate, the peak of epidemic situation will gradually decrease. When the failure rate is less than 0.01, the peak time will advance with the decrease of failure rate; when the failure rate is greater than 0.01, the peak time will be delayed with the decrease of failure rate. If only Figures 6 and 7 are used to illustrate that 0.01 is the boundary value of peak time trend change, it may be coincidental because the failure rate less than 0.01 is taken as the step of 0.001, and the failure rate greater than 0.01 is taken as the step of 0.01. Therefore, we further take the failure rate from 0.01 to 0.02 in steps of 0.001 for simulation, as shown in Figure 8. It can be seen from Figure 8 that the time of peak value is delayed with the decrease of failure efficiency. In general, when the step of failure rate change is 0.001, the simulation shows that when the fixed vaccination rate is 0.005, the peak of epidemic situation will decrease with the decrease of failure efficiency. When the failure rate is less than 0.01, the peak time will advance with the decrease of failure efficiency; when the failure rate is greater than 0.01, the peak time will be delayed with the decrease of failure efficiency.

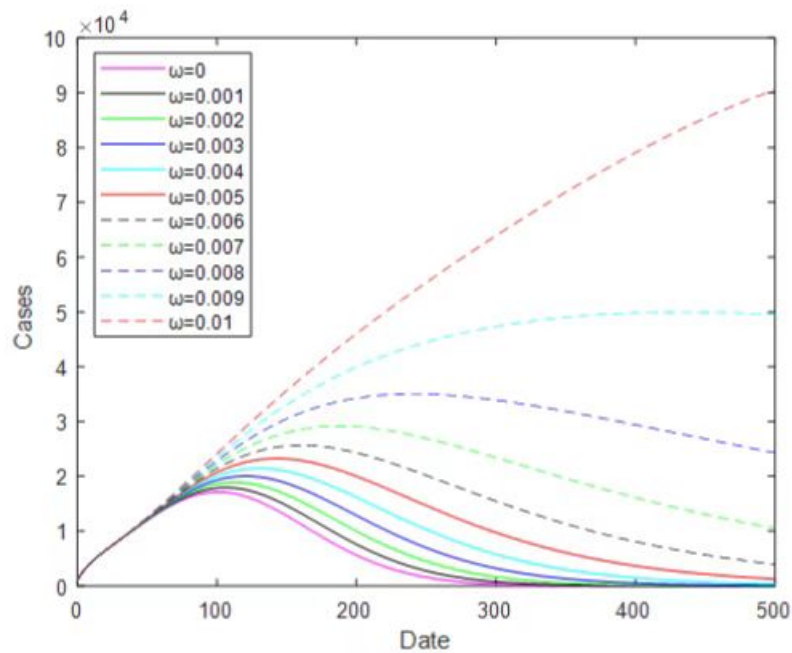


Figure 6. The number of infected cases under different vaccine failure rates when the vaccination rate is 0.005 (failure rates are taken from 0 to 0.01 in steps of 0.001).

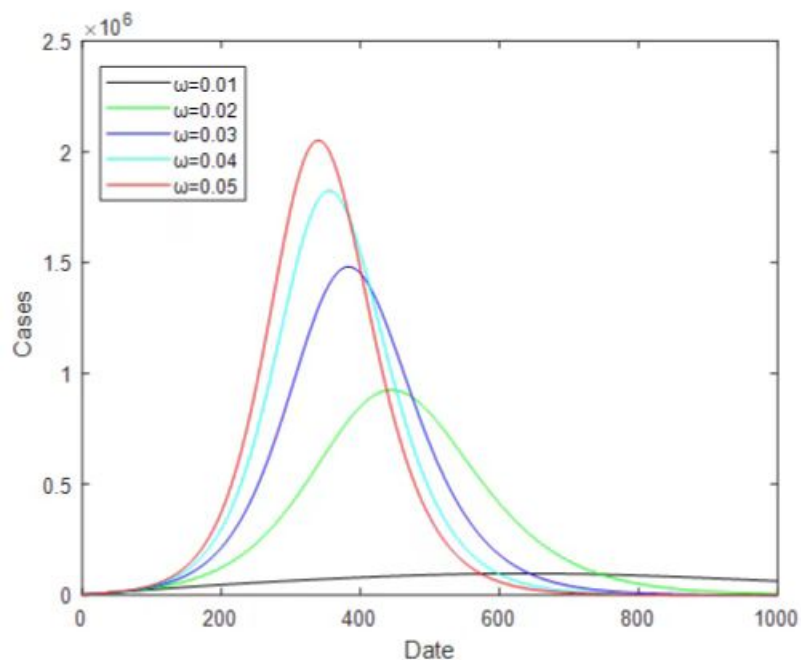


Figure 7. The number of infected cases under different vaccine failure rates when the vaccination rate is 0.005 (failure rates are taken from 0.01 to 0.05 in steps of 0.01).

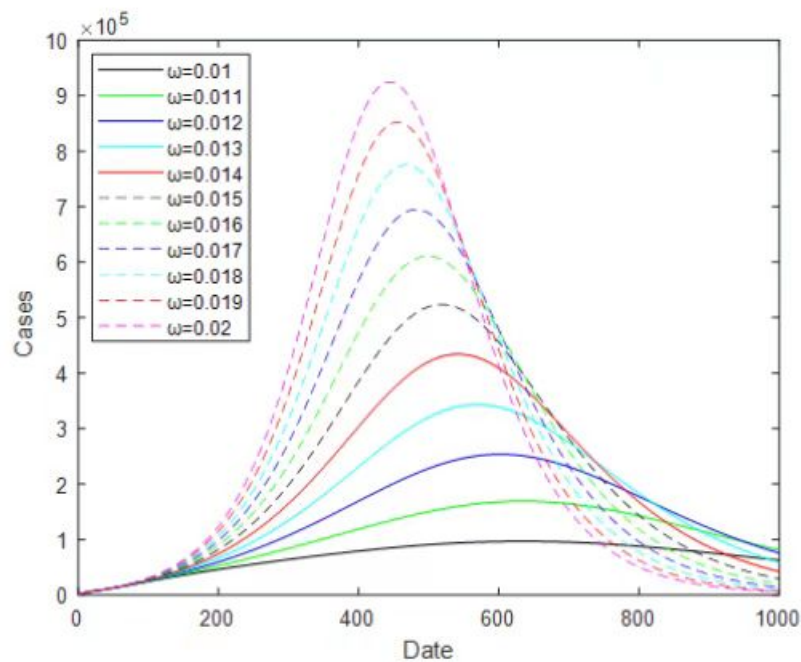


Figure 8. The number of infected cases under different vaccine failure rates when the vaccination rate is 0.005 (failure rates are taken from 0.01 to 0.02 in steps of 0.001).

When the vaccination rate is 0.005, the line chart of the epidemic peak under different vaccine failure rates is shown in Figure 9. When the value of failure rate is large (greater than 0.02), the peak will increase significantly. When the failure rate is 0.001 the peak value is 81.4% lower than the peak value when the failure rate is 0.01, and when the failure rate is 0.01 the peak value is 89.5% lower than the peak value when the failure rate is 0.02. Therefore, the lower the vaccine failure rate, the lower the peak of the epidemic. The peak values under different failure rates are shown in Table 2.

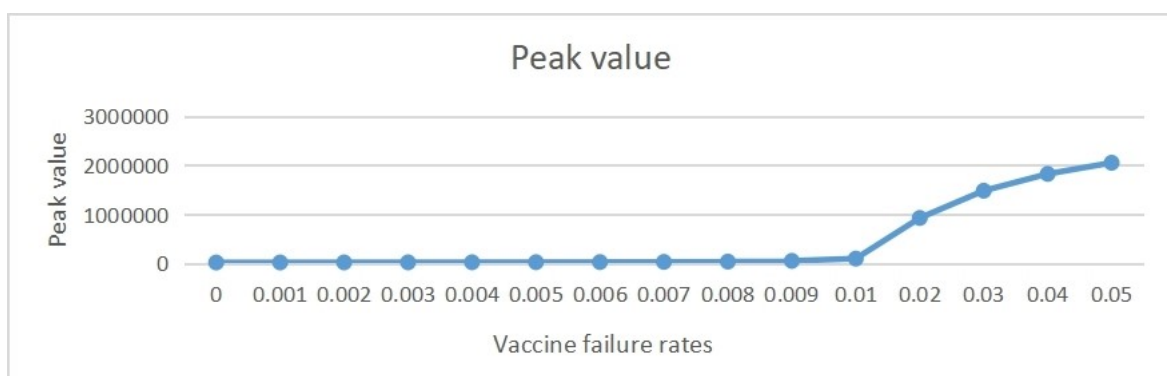


Figure 9. The peak value of infected cases under different vaccine failure rates when the vaccination rate is 0.005.

When the vaccination rate is 0.005, the line chart of the peak time of epidemic situation under

different vaccine failure rates is shown in Figure 10. It can be seen when the failure rate is less than 0.01, the peak time will advance with the decrease of failure rate; when the failure rate is greater than 0.01, the peak time will be delayed with the decrease of failure rate. When the failure rate is 0.01, the peak time is 528 days later than that when the failure rate is 0.001 and 295 days later than that when the failure rate is 0.05. The peak time under different failure rates is shown in Table 2.

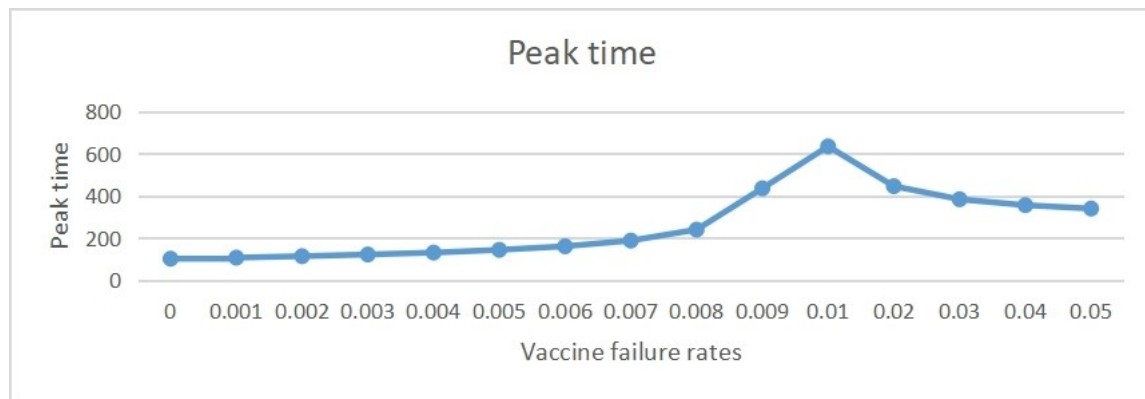


Figure 10. The peak time of infected cases under different vaccine failure rates when the vaccination rate is 0.005.

Table 2. Peak value and peak time of infected cases and vaccine effective time period under different vaccine failure rates when the vaccination rate is 0.005.

Vaccine failure rates	Vaccine effective time period (days)	Peak value	Peak time (days)
0	FOREVER	17126	101
0.001	1000	17934	106
0.002	500	18887	113
0.003	333	20032	121
0.004	250	21443	130
0.005	200	23244	143
0.006	167	25658	160
0.007	143	29159	187
0.008	125	35046	239
0.009	111	49967	435
0.01	100	96669	634
0.02	50	924,980	445
0.03	33	1,481,000	383
0.04	25	1,823,700	355
0.05	20	2,050,800	339

We also discuss the number of new cases per day at 30, 40, 50, 60 and 70 days in England with

different failure rates when the vaccination rate is 0.005. The results are shown in Figure 11. It can be seen from the figure that at the same time, the smaller the failure rate, the fewer the number of cases. On the 60th day of vaccination, the vaccine with failure rate of 0.002 is 5.8% lower than the vaccine with failure rate of 0.01; on the 70th day of vaccination, the vaccine with failure rate of 0.002 is 9.1% lower than the vaccine with failure rate of 0.01. Therefore, with the extension of time, the vaccine with low failure rate is more effective in reducing the number of cases than the vaccine with high failure rate. The number of cases is shown in Table 3.

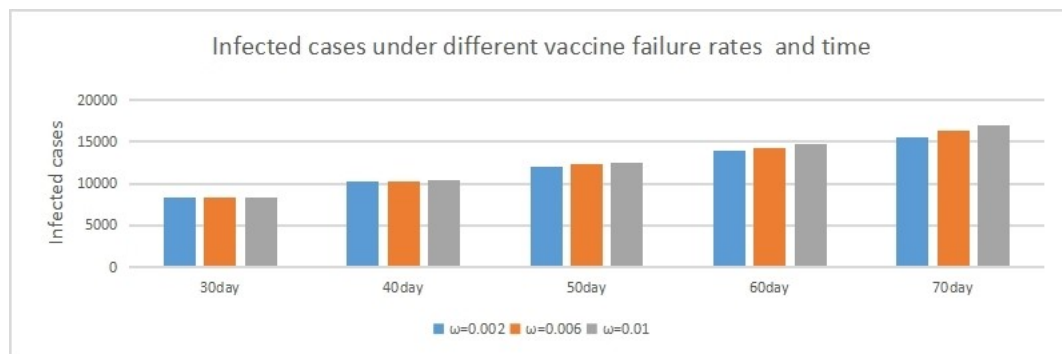


Figure 11. Infection cases under different vaccine failure rates at 30 days, 40 days, 50 days, 60 days and 70 days when the vaccination rate is 0.005 (The blue histogram means the vaccine failure rate is 0.002; the orange histogram means the vaccine failure rate is 0.006; the grey histogram means the failure rate is 0.01).

Table 3. Infection cases under different vaccine failure rates at 30 days, 40 days, 50 days, 60 days and 70 days when the vaccination rate is 0.005.

	30 days	40 days	50 days	60 days	70 days
$\omega = 0.002$	8337	10214	12079	13862	15476
$\omega = 0.006$	8366	10305	12298	14307	16276
$\omega = 0.010$	8393	10390	12502	14720	17020

When the vaccination rate is 0.01, we discuss the impact of different vaccine failure rates on the spread of the epidemic in England, the results are shown in Figures 12–15. The simulation results show that the smaller the failure rate is, the lower the peak of epidemic situation is, and 0.019 is the boundary value of failure rate. When the failure rate is less than 0.019, the peak time will advance with the decrease of failure rate; when the failure rate is greater than 0.019, the peak time will be delayed with the decrease of failure rate. Some data are shown in Table 4.

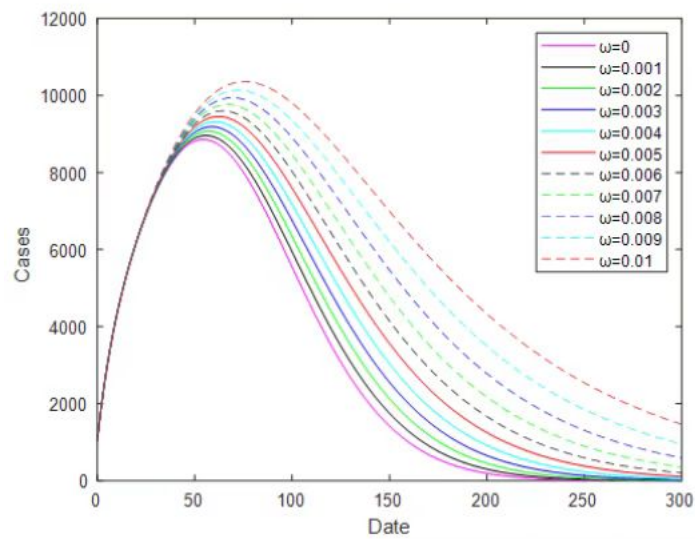


Figure 12. The number of infected cases under different vaccine failure rates when the vaccination rate is 0.01 (failure rates are taken from 0 to 0.01 in steps of 0.001).

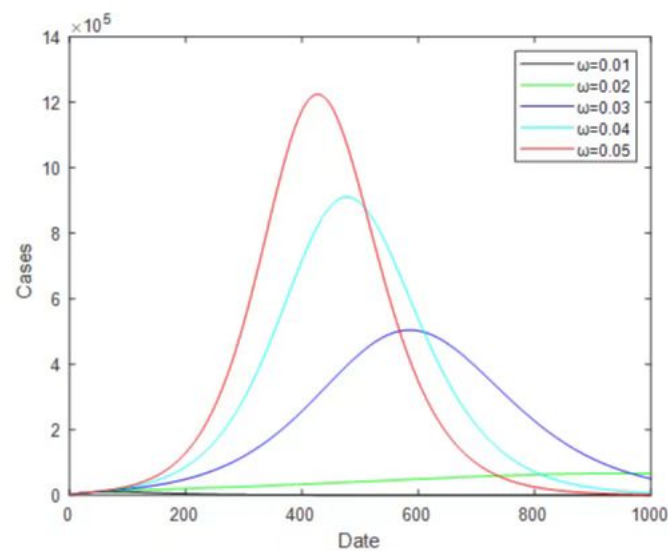


Figure 13. The number of infected cases under different vaccine failure rates when the vaccination rate is 0.01 (failure rates are taken from 0.01 to 0.05 in steps of 0.01).

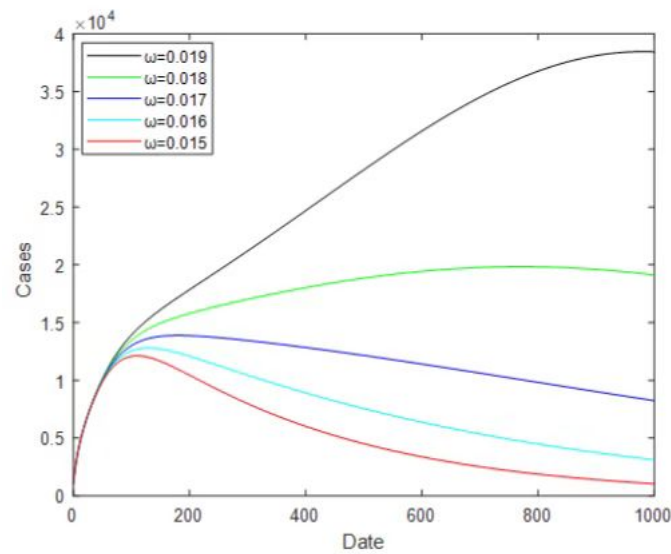


Figure 14. The number of infected cases under different vaccine failure rates when the vaccination rate is 0.01 (failure rates are taken from 0.015 to 0.019 in steps of 0.001).

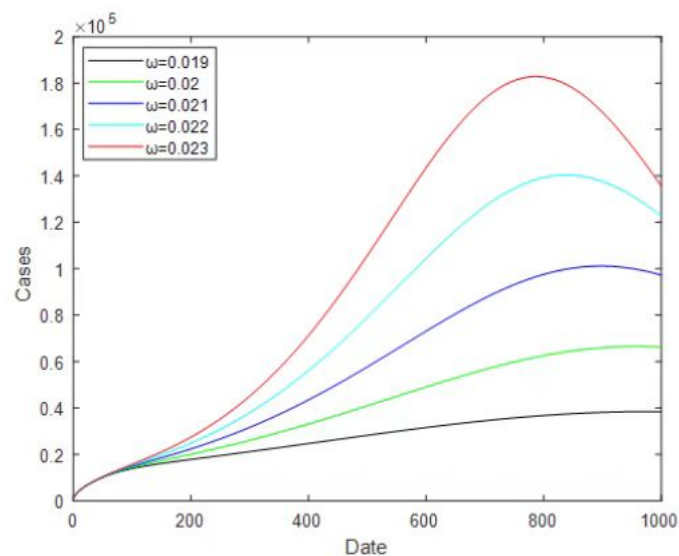


Figure 15. The number of infected cases under different vaccine failure rates when the vaccination rate is 0.01 (failure rates are taken from 0.019 to 0.023 in steps of 0.001).

Table 4. Peak value and peak time of infected cases under different vaccine failure rates when the vaccination rate is 0.01.

failure rates	0	0.005	0.01	0.015	0.019	0.02	0.021
Peak value	8856	9452	10354	12125	38455	66507	101150
Peak time (days)	54	62	75	110	979	956	892

4.3. Effects of different vaccination rates on the epidemic situation in England

When the vaccine failure rate is 0.005, the impact of different vaccination rates on the spread of the epidemic in England is shown in Figure 16. The vaccination rates change from 0.005 to 0.025 in steps of 0.005. According to the simulation, the peak of epidemic situation decreases with the increase of vaccination rate, and the peak time advances with the increase of vaccination rate. When the vaccination rate is 0.025, the peak value decrease by 74.8% and the peak time is 114 days earlier than that when the vaccination rate is 0.005. The result is given in Table 5.

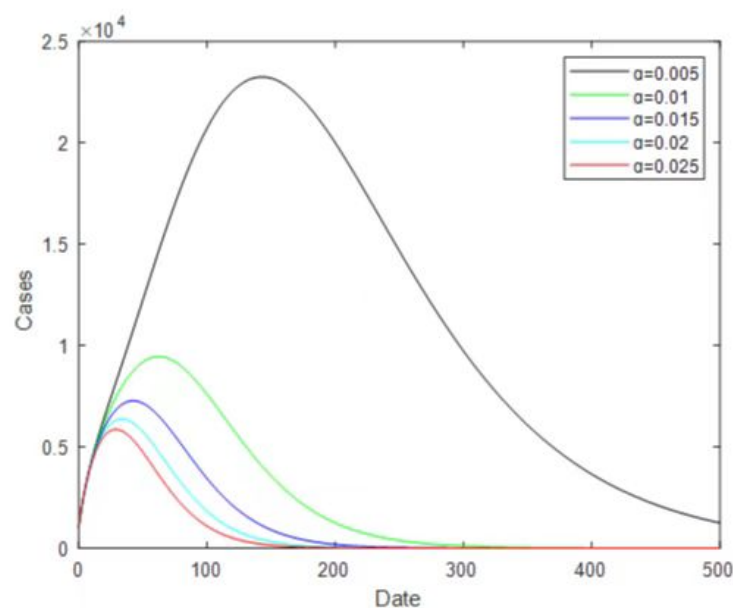


Figure 16. The number of infected cases under different vaccination rates when the vaccine failure rate is 0.005 (the vaccination rates are taken from 0.005 to 0.025 in steps of 0.005).

Table 5. Peak value and peak time of infected cases under different vaccination rates when the vaccine failure rate is 0.005.

Vaccination rate	0.005	0.01	0.015	0.02	0.025
Peak value	23244	9452	7269	6370	5857
Peak time (days)	143	62	42	34	29

In order to comprehensively evaluate the effects of vaccination rate and failure rate on the peak infection cases and peak time, we add heat-maps for peak infection cases and peak times, the results are shown in Figures 17 and 18. The vaccination rates change from 0.002 to 0.005 in steps of 0.001 and the vaccine failure rates change from 0.001 to 0.01 in steps of 0.001.

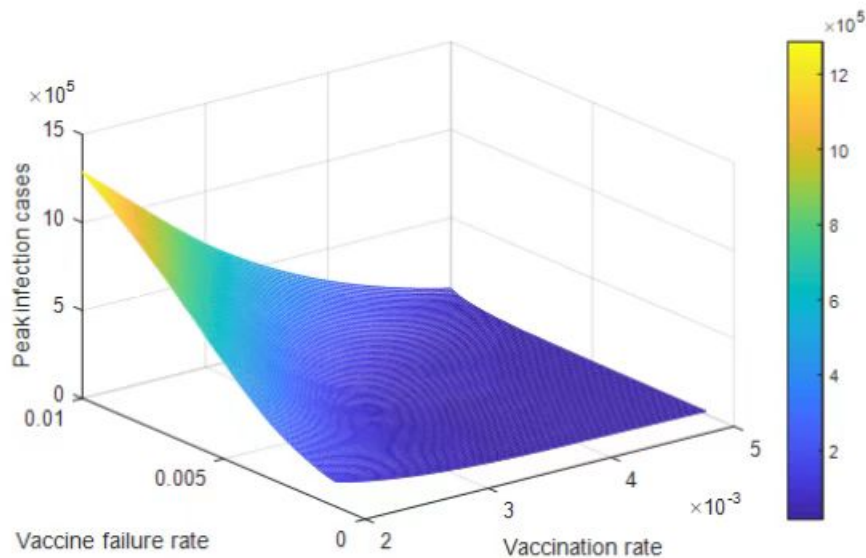


Figure 17. The peak infection cases under different vaccination rates and vaccine failure rates.

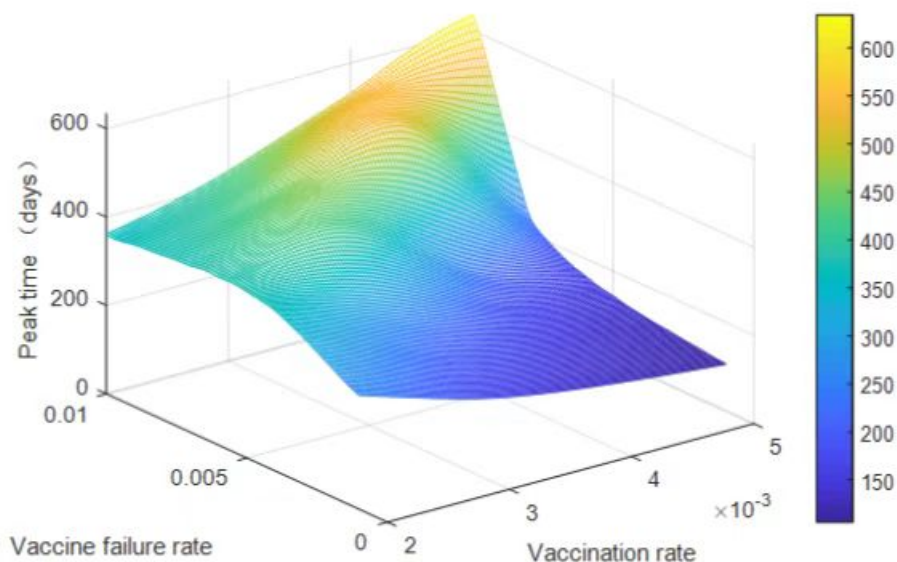


Figure 18. The peak time of infected cases under different vaccination rates and vaccine failure rates.

5. Conclusions

The first part of this study is to develop an improved SEIR model of COVID-19 transmission in England taking into account the decline in antibody levels in recovers. In the second part, a SEIRV vaccination model is established on the basis of the decline in antibody levels, taking into account that susceptible populations are vaccinated at a fixed vaccination rate every day. We calculate the basic reproduction number of model (2.1) and the control reproduction number of model (3.1), calculate the disease-free equilibrium point and endemic equilibrium point of the two models, and analyze the stability of the model.

In the numerical simulation part, we further explain the vaccination rate and failure rate: $\alpha = 0.005$ means that 250,000 people are vaccinated every day on the basis of 50 million people in England, on the basis of this vaccination rate, the overall immunization rate is 25.9% after 60 days of continuous vaccination. In addition, the meaning of vaccine failure rate ω refers to the reciprocal of the duration of vaccine effectiveness, that is, each corresponds to a duration of vaccine effectiveness.

In model (3.1), we investigate the impact of different failure rates on the spread of the epidemic in England when the vaccination rates are 0.005 and 0.01. The results shows that when the fixed vaccination rate is 0.005, when the failure rate is 0.001, the peak value is 81.4% lower than that when the failure rate is 0.01, and when the failure rate is 0.01 the peak value is 89.5% lower than that when the failure rate is 0.02. In addition, when the failure rate is 0.01, the peak time is 528 days later than when the failure rate is 0.001 and 295 days later than when the failure rate is 0.05. Therefore, the peak of epidemic situation will decrease with the decrease of failure efficiency. The peak time of the epidemic has two situations. When the failure rate is less than 0.01, the peak time will advance with the decrease of failure efficiency; when the failure rate is greater than 0.01, the peak time will be delayed with the decrease of failure efficiency. On the 60th day of vaccination, the vaccine with failure rate of 0.002 is 5.8% lower than the vaccine with failure rate of 0.01, on the 70th day of vaccination, the vaccine with failure rate of 0.002 is 9.1% lower than the vaccine with failure rate of 0.01. Therefore, with the extension of time, the vaccine with low failure rate is more effective in reducing the number of cases than the vaccine with high failure rate. When the fixed vaccination rate is 0.01, the peak of epidemic situation will decrease with the decrease of failure efficiency. When the failure rate is less than 0.019, the peak time will advance with the decrease of failure efficiency; when the failure rate is greater than 0.019, the peak time will be delayed with the decrease of failure efficiency. We also investigate the impact of different vaccination rates on the spread of the epidemic in England when the fixed vaccine failure rate is 0.005. The peak of epidemic situation decreases with the increase of vaccination rate, and the peak time is advanced with the increase of vaccination rate. When the vaccination rate is 0.025, the peak value decreases by 74.8% and the peak time is 114 days earlier than that when the vaccination rate was 0.005.

6. Discussion

The rationality of the fitting value of $P = 1.8888 \times 10^{-6}$. This fitting value refers to the level of antibody decline in the actual recovered patients, including not only the number of hospitalizations officially counted, but also the number of uncounted patients with moderate and mild symptoms, and the number of confirmed asymptomatic infections. This value is somewhat underestimated. If only the

number of recovered patients in hospital is counted according to official data from the UK government, this fitted value may have practical significance. Antibody levels take longer to drop due to higher antibody levels in severely recovered patients [26].

In model (3.1), the meaning of the vaccine failure rate refers to the inverse of the effective duration of the vaccine, that is, the failure rate corresponds to the effective duration of an effective vaccine. The data details are shown in Table 1. Similarly, the vaccination rate corresponds to a time period in which vaccinations are completed, for example $\alpha = 0.005$ indicating that it takes 200 days to complete all vaccinations.

In the numerical simulation part, the peak always decreases as the vaccine failure rate decreases. Peak arrival times may be related to boundary values. When the failure rate is less than the boundary value, the peak time will advance as the failure rate decreases; when the failure rate is greater than the boundary value, the peak time will be delayed as the failure rate decreases. In this study, when the vaccination rate was 0.005, the boundary value for the failure rate was 0.01; when the vaccination rate was assumed to be 0.01, the boundary value for the failure rate was 0.019. The boundary values in this paper are based on the failure rate with a step size of 0.001, when we take a smaller step size for simulation, we may get more accurate failure rate boundary values.

Israel has one of the highest vaccination rates in the world [27]. On December 20, 2020, the country took the lead in launching the world's first universal vaccination program for COVID-19. According to the official website of the Israeli Ministry of Health [28], as of March 2, 2020, the proportion of Israel receiving one dose of the vaccine was 51.67%, and the proportion of receiving two doses of the new crown vaccine was 37.53%. By early August 2021, about 62% of Israel's 9.3 million population had received at least one dose of the vaccine, and about 58% had completed two doses. Israel, despite reaching such a high vaccination rate, saw a new peak of cases in early September 2021. According to the World Health Organization, on September 1, 2021, Israel recorded more than 10,000 new cases per day. By the end of August 2021, the vaccination rate in Singapore had reached 80%, and since September 2021, the number of new cases in Singapore has increased significantly, and by the end of October, there were more than 5,000 new cases in a single day.

This article explores the impact of different vaccine failure rates on the spread of the COVID-19 outbreak in the UK, given a certain vaccination rates. Although many countries have achieved high vaccination rates, and even theoretically achieved rates of herd immunity, from the data alone, vaccination does not seem to have a significant inhibitory effect on the epidemic in these countries. The reason may be that the mutated virus is difficult to deal with, or the vaccine is not as effective as expected. In the next article, we will use data from severe cases to assess vaccine efficacy and protection. Vaccination rates can be increased through government policies, but if the protection rate of the vaccine itself is not high, increasing the vaccination rate will not help to fundamentally control the epidemic.

Acknowledgments

This study was funded by Natural Science Foundation of China (NSFC 11901027, 11871093), the China Postdoctoral Science Foundation(2021M703426), Postgraduate Teaching Research and Quality Improvement Project of BUCEA (J2021010), BUCEA Post Graduate Innovation Project (2021098, 2021099). We thank all the individuals who generously shared their time and materials for this study.

Conflict of interest

The authors declare there is no conflict of interest.

References

1. D. Wang, B. Hu, C. Hu, F. Zhu, X. Liu, J. Zhang, et al., Clinical characteristics of 138 hospitalized patients with 2019 novel coronavirus–infected pneumonia in Wuhan, China, *JAMA*, **323** (2020), 1061–1069. <https://doi.org/10.1001/jama.2020.1585>
2. N. Zhu, D. Zhang, W. Wang, X. Li, B. Yang, J. Song, et al., A novel coronavirus from patients with pneumonia in China, 2019, *N. Engl. J. Med.*, **382** (2020), 727–733. <https://doi.org/10.1056/NEJMoa200101>
3. T. Guo, Q. Shen, W. Guo, W. He, J. Li, Y. Zhang, et al., Clinical characteristics of elderly patients with Covid-19 in Hunan province, China: a multicenter, retrospective study, *Gerontology*, **66** (2020), 1–9. <https://doi.org/10.1159/000508734>
4. UCLA, *Scientists Discover How COVID-19 Virus Causes Multiple Organ Failure in Mice*, 2020. Available from: <https://newsroom.ucla.edu/releases/covid-19-multiple-organ-failure-systemic-effects>.
5. World Health Organization, *WHO Coronavirus (COVID-19) Dashboard*, 2021. Available from: <https://covid19.who.int/>.
6. GOV.UK, *Coronavirus (COVID-19) in the UK*, 2020. Available from: <https://coronavirus.data.gov.uk/details/cases>.
7. Imperial College London, *Coronavirus Antibody Prevalence Falling in England, REACT Study Shows*, 2021. Available from: <https://www.imperial.ac.uk/news/207333/coronavirus-antibody-prevalence-falling-england-react/>.
8. Q. Long, X. Tang, Q. Shi, Q. Li, H. Deng, J. Yuan, et al., Clinical and immunological assessment of asymptomatic SARS-CoV-2 infections, *Nat. Med.*, **26** (2020), 1200–1204. <https://doi.org/10.1038/s41591-020-0965-6>
9. J. Seow, C. Graham, B. Merrick, S. Acors, S. Pickering, K. J. A. Steel, et al., Longitudinal observation and decline of neutralizing antibody responses in the three months following SARS-CoV-2 infection in humans, *Nat. Microbiol.*, **5** (2020), 1598–1607. <https://doi.org/10.1038/s41564-020-00813-8>
10. P. Mlcochova, S. Kemp, M. S. Dhar, G. Papa, B. Meng, S. Mishra, et al., SARS-CoV-2 B.1.617.2 Delta variant replication and immune evasion, *Nature*, **599** (2021), 114–119. <https://doi.org/10.1038/s41586-021-03944-y>
11. P. D. Yadav, G. N. Sapkal, E. Raches, R. R. Sahay, D. A. Nyayanit, D. Y. Patil, et al., Neutralization of Beta and Delta variant with sera of COVID-19 recovered cases and vaccines of inactivated COVID-19 vaccine BBV152/Covaxin, *J. Travel. Med.*, **28** (2021), 1195–1982. <https://doi.org/10.1093/jtm/taab104>

12. D. Planas, D. Veyer, A. Baidaliuk, I. Staropoli, F. Guivel-Benhassine, M. M. Rajahet, et al., Reduced sensitivity of SARS-CoV-2 variant Delta to antibody neutralization, *Nature*, **596** (2021), 276–280. <https://doi.org/10.1038/s41586-021-03777-9>
13. P. Wintachai, K. Prathom, Stability analysis of SEIR model related to efficiency of vaccines for COVID-19 situation, *Heliyon*, **7** (2021), e06812. <https://doi.org/10.1016/j.heliyon.2021.e06812>
14. A. Fuady, N. Nuraini, K. K. Sukandar, B. W. Lestari, Targeted vaccine allocation could increase the COVID-19 vaccine benefits amidst its lack of availability: A mathematical modeling study in Indonesia, *Vaccines*, **9** (2021), 050462. <https://doi.org/10.3390/VACCINES9050462>
15. M. Angeli, G. Neofotistos, M. Mattheakis, E. Kaxiras, Modeling the effect of the vaccination campaign on the COVID-19 pandemic, *Chaos, Solitons Fractals*, **154** (2022), 111621. <https://doi.org/10.1016/j.chaos.2021.111621>
16. S. Zhai, G. Luo, T. Huang, X. Wang, J. Tao, P. Zhou, Vaccination control of an epidemic model with time delay and its application to COVID-19, *Nonlinear Dyn.*, **106** (2021), 1279–1292. <https://doi.org/10.1007/s11071-021-06533-w>
17. J. Medina, R. Cessa-Rojas, V. Umpaichitra, Reducing COVID-19 cases and deaths by applying blockchain in vaccination rollout management, *IEEE Open J. Engineer. Med. Biol.*, **2** (2021), 249–255. <https://doi.org/10.1109/OJEMB.2021.3093774>
18. A. Karabay, A. Kuzdeuov, S. Ospanova, M. Lewis, H. A. Varol, A vaccination simulator for COVID-19: Effective and sterilizing immunization cases, *IEEE J. Biomed. Health Inf.*, **25** (2021), 4317–4327. <https://doi.org/10.1109/JBHI.2021.3114180>
19. 25th International Conference on System Theory, Control and Computing (ICSTCC), *Simulation of SARS-CoV-2 Pandemic in Germany with Ordinary Differential Equations in MATLAB*, 2021. Available from: <https://doi.org/10.1109/ICSTCC52150.2021.9607181>.
20. H. Chen, B. Haus, P. Mercorelli, Extension of SEIR compartmental models for constructive Lyapunov control of COVID-19 and analysis in terms of practical stability, *Mathematics*, **9** (2021), 172076. <https://doi.org/10.3390/math9172076>
21. P. V. D. Driessche, Reproduction numbers of infectious disease models, *Infect. Dis. Model.*, **2** (2017), 288–303. <https://doi.org/10.3390/math9172076>
22. Y. Zhang, C. You, Z. Cai, J. Sun, W. Hu, X. Zhou, et al., Prediction of the COVID-19 outbreak based on a realistic stochastic model, preprint: <https://doi.org/10.1101/2020.03.10.20033803>.
23. Irish Examiner, *Covid-19 Vaccination ‘Incubation Period’ for 10-14 Days before Second Dose*, 2020. Available from: <https://www.irishexaminer.com/world/arid-40198611.html>.
24. The Emory Wheel, *COVID-19 Cases Remain Steady after Two Weeks Mask Optional*, 2022. Available from: <https://emorywheel.com/covid-19-cases-remain-steady-after-two-weeks-mask-optional>.
25. D. F. Gudbjartsson, G. L. Norddahl, P. Melsted, K. Gunnarsdottir, K. Stefansson, Humoral immune response to SARS-CoV-2 in iceland, *New Engl. J. Med.*, **383** (2020), 1724–1734. <https://doi.org/10.1056/NEJMoa2026116>

26. A. Longchamp, J. Longchamp, A. Croxatto, G. Greub, J. Delaloye, Serum antibody response in critically ill patients with COVID-19, *Intensive Care Med.*, **46** (2020), 1921–1923. <https://doi.org/10.1007/s00134-020-06171-7>
27. GOV.CHN, *News Analysis: As lockdown extends, Israel Faces Dilemma on How to Move Forward* World Knowledge, 2021. Available from: http://www.china.org.cn/world/Off_the_wire/2020-03/31/content_75878980.htm.
28. Worldometer, *WORLD/COUNTRIES/ISRAEL*, 2021. Available from: <https://www.worldometers.info/coronavirus/country/israel/>.



AIMS Press

© 2022 the Author(s), licensee AIMS Press. This is an open access article distributed under the terms of the Creative Commons Attribution License (<http://creativecommons.org/licenses/by/4.0>)